Satellite Products and Services Review Board

Algorithm Theoretical Basis Document: ASCAT Ultra High Resolution (UHR) Wind Direction Quality Control via Computer Vision Techniques

Compiled by:
NOAA/NESDIS/STAR Ocean Surface Winds Team

Version 1.0

April, 2026

AUTHORS:

Matthew McKinney (Global Science & Technology): *matthew.mckinney@noaa.gov*
Seubson Soisuvarn (UCAR): *seubson.soisuvarn@noaa.gov*
Zorana Jelenak (UCAR): *zorana.jelenak@noaa.gov*
Paul S. Chang (NOAA/NESDIS/STAR): *paul.s.chang@noaa.gov*

DOCUMENT HISTORY DOCUMENT REVISION LOG

DOCUMENT TITLE: ATBD – ASCAT UHR Wind Direction QC			
DOCUMENT CHANGE HISTORY			
Revision No.	**Date**	**Description**	**Author**
1.0	04/2026	Initial Release	M. McKinney

Table of Contents

LIST OF ACRONYMS

LIST OF ACRONYMS

Acronym	Definition
ASCAT	Advanced Scatterometer
ATBD	Algorithm Theoretical Basis Document
CMOD	C-band Model Function
GMF	Geophysical Model Function
IBTrACS	International Best Track Archive for Climate Stewardship
MLE	Maximum Likelihood Estimator
NESDIS	National Environmental Satellite, Data, and Information Service
NOAA	National Oceanic and Atmospheric Administration
NRCS	Normalized Radar Cross Section
QC	Quality Control
RBF	Radial Basis Function
SNR	Signal-to-Noise Ratio
STAR	Center for Satellite Applications and Research
TC	Tropical Cyclone
UHR	Ultra High Resolution
WVC	Wind Vector Cell

Section 1
Introduction and Instrument Background

1.1. Purpose

This Algorithm Theoretical Basis Document (ATBD) describes the quality control algorithms developed for the Advanced Scatterometer (ASCAT) Ultra High Resolution (UHR) ocean surface wind vector product. The algorithms employ computer vision techniques to detect and correct anomalous wind direction retrievals that arise from the inherent ambiguity resolution challenges in scatterometer data processing.

The ASCAT UHR wind product provides ocean surface wind vectors at approximately 1.0 to 2.5 km resolution, a significant improvement over the standard 12.5 km and 25 km products (Lindsley, 2010) (Soisuvarn, High-Resolution Coastal Winds From the NOAA Near Real-Time ASCAT Processor, 2023). However, the increased spatial resolution introduces additional noise in the wind direction field, particularly in regions of strong wind direction gradients such as tropical cyclone environments. This document details the mathematical foundations, algorithmic procedures, and implementation specifics of the quality control framework.

1.2. Scope

This ATBD covers the following algorithmic components of the ASCAT UHR wind direction quality control system: (Section 2) The mathematical foundations necessary to understand the framework; (Section 3) anomaly detection using contour-based spatial filtering with connected component analysis; (Section 4) circular interpolation of flagged wind directions using complex exponential representations; (Section 5) wind direction ambiguity re-selection using angular distance minimization; (Section 6) wind speed retrieval via the CMOD5.h Geophysical Model Function (GMF); and (Section 7) iterative convergence processing to progressively refine the wind field.

1.3. ASCAT Instrument Overview

ASCAT is a real-aperture radar scatterometer operating at C-band (5.255 GHz) aboard the MetOp series of polar-orbiting satellites operated by EUMETSAT. The instrument illuminates the ocean surface from three fixed fan-beam antennas: a fore beam, a mid beam, and an aft beam. Each antenna provides a normalized radar cross section (NRCS, or σ_0) measurement at a different azimuth angle relative to the satellite ground track (EUMETSAT, 2014).

The ASCAT UHR product is generated by processing the full-resolution backscatter data to achieve wind vector cells (WVCs) at 1.0 to 2.5 km resolution, compared to the operational 12.5 km product (Soisuvarn, High-Resolution Coastal Winds From the NOAA Near Real-Time ASCAT Processor, 2023). The three independent σ_0 measurements at each WVC enable wind vector retrieval through inversion of a Geophysical Model Function (GMF), which relates wind

speed, wind direction relative to the antenna azimuth, and incidence angle to the expected NRCS value.

The wind retrieval process produces up to four ambiguous wind direction solutions at each WVC. An ambiguity removal step, typically based on a two-dimensional variational analysis method (2DVAR) or median filter, selects the most likely solution. However, at UHR resolution, the reduced spatial averaging and higher noise levels can lead to incorrect ambiguity selections, manifesting as spatially incoherent wind direction patterns. The algorithms described in this document address these artifacts through a post-processing quality control framework.

Section 2
Mathematical Foundations

2.1. Circular Statistics for Wind Directions

Wind directions are circular (angular) quantities defined on the interval [0°, 360°), where 0° and 360° represent the same direction. Standard linear arithmetic operations (e.g., averaging, differencing, interpolation) are not directly applicable to circular data due to the discontinuity at the 0°/360° boundary. This section describes the mathematical framework used throughout the quality control algorithms to handle circular wind direction data.

2.1.1. Euler's Formula Representation

The fundamental approach to handling circular wind directions is to represent each angle as a point on the unit circle in the complex plane using Euler's formula:

$$z = \exp(i\theta) = cos(\theta) + i\,sin(\theta) \tag{1}$$

where θ is the wind direction in radians. This mapping transforms the circular domain to the complex plane, where standard arithmetic operations are well-defined. The implementation converts degrees to radians before applying the exponential: z = exp(i · π/180 · α), where α is the wind direction in degrees.

2.1.2. Circular Mean

The circular mean of a set of N wind directions $\{\theta_1, \theta_2, ..., \theta_n\}$ is computed by averaging their complex exponential representations and converting back to degrees:

$$\bar{a} = atan2\big(\mathrm{Im}(\bar{z}), \mathrm{Re}(\bar{z})\big), \quad \text{where } \bar{z} = \frac{1}{N}\sum_{k=1}^{N} z_k = \frac{1}{N}\sum_{k=1}^{N} \exp i\theta_k \tag{23}$$

This approach correctly handles the circular discontinuity; for example, the mean of 350° and 10° is correctly computed as 0° rather than 180°. atan2 is an arctan function in numpy that is designed to handle discontinuity and preserve direction.

2.1.3. Circular Difference

The signed angular difference between two directions a and b is defined as:

$$\Delta\alpha = \big((a - b + 180)\ mod\ 360\big) - 180 \tag{45}$$

This yields values in the range [–180°, 180°]. The unsigned (absolute) difference is |Δα|, representing the shortest angular distance between two directions.

2.1.4. Circular Quantiles

Quantile computation for circular data requires special treatment. The algorithm computes the center of mass (average) of the complex exponential representations, then calculates signed

differences from this center. The resulting linear differences are sorted, and standard quantile indices are applied. This approach avoids linear representation errors from the 0°/360° discontinuity when computing percentiles. The quantile range (q-range) is defined as the absolute difference between the specified upper and lower quantile values in the sorted circular-difference space.

2.2. Local Spatial Operators

2.2.1. Sliding Window (3×3)

A 3×3 sliding window operator is implemented using NumPy stride tricks for efficient extraction of local neighborhoods. The input array is padded with NaN values along each edge (by 1 cell for a 3×3 window), and a view into the strided memory is created without data copying. The resulting flattened windows provide 9-element vectors for each grid cell, with the center element at index 4.

2.2.2. Maximum Local Wind Direction Difference

For each wind vector cell (WVC), the maximum angular difference between the center cell's wind direction and all 8 surrounding cells is computed:

$$D(i,j) = max\left|\Delta\alpha\left(WVC(i,j), WVC(i+m, j+n)\right)\right| : m,n \in -1,0,1 \quad (6)$$

This quantity serves as the primary discriminant for identifying directional discontinuities. Cells with high D values indicate locations where the wind direction changes abruptly, characteristic of ambiguity selection errors.

Section 3
Anomaly Detection Algorithm

3.1. Algorithm Overview

The anomaly detection algorithm identifies spatially incoherent wind direction patterns using a contour-based approach inspired by computer vision techniques. The algorithm proceeds through six sequential stages: (1) computation of local directional differences, (2) negative thresholding to identify regions of directional agreement, (3) connected component labeling to group contiguous agreement regions into objects, (4) statistical characterization of each object and its boundary, (5) verification tests to classify objects as consistent or anomalous, and (6) generation of a binary quality control mask.

3.2. Cardinal Difference Computation

For each WVC in the 2D wind direction field, the maximum local wind direction difference D(i,j) is computed using the 3×3 sliding window operator described in Section 2.2.2. This produces a scalar field where large values indicate locations of directional discontinuity and small values indicate regions of directional agreement (see Figure 1).

3.3. Negative Thresholding

A binary mask is generated by applying a configurable threshold τ_{diff} (default: 7.5°) to the cardinal difference field:

$$T(i,j) = \begin{cases} 1, & D(i,j) < \tau_{diff} \\ 0, & \text{otherwise} \end{cases} \quad (7)$$

This is termed "negative thresholding" because the mask identifies a photo negative of the edges (regions of discontinuity) which it is intended to detect. The threshold value of 7.5° was empirically determined to capture the typical noise level in ASCAT UHR wind direction retrievals while preserving genuine meteorological gradients.

3.4. Connected Component Labeling

The binary agreement mask T is processed using SciPy's connected component labeling algorithm (scipy.ndimage.label), which assigns a unique integer label to each contiguous group of True-valued cells. Each labeled region represents a spatially connected area where neighboring wind directions agree to within the threshold. These labeled objects are the fundamental units of analysis for the subsequent verification steps.

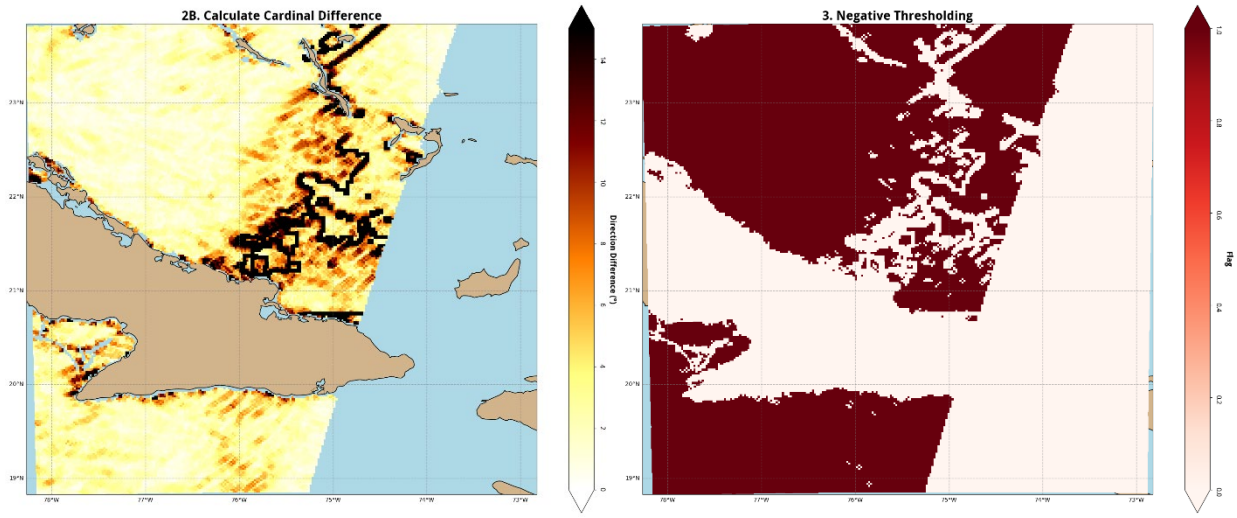

Figure 1 ASCAT-B pass over Melissa on October 29th, 2025. (Left) The values represent the cardinal difference operator explained in section 3.2. (Right) The values represent the binary mask as described in the "Negative Threshold" technique in section 3.3.

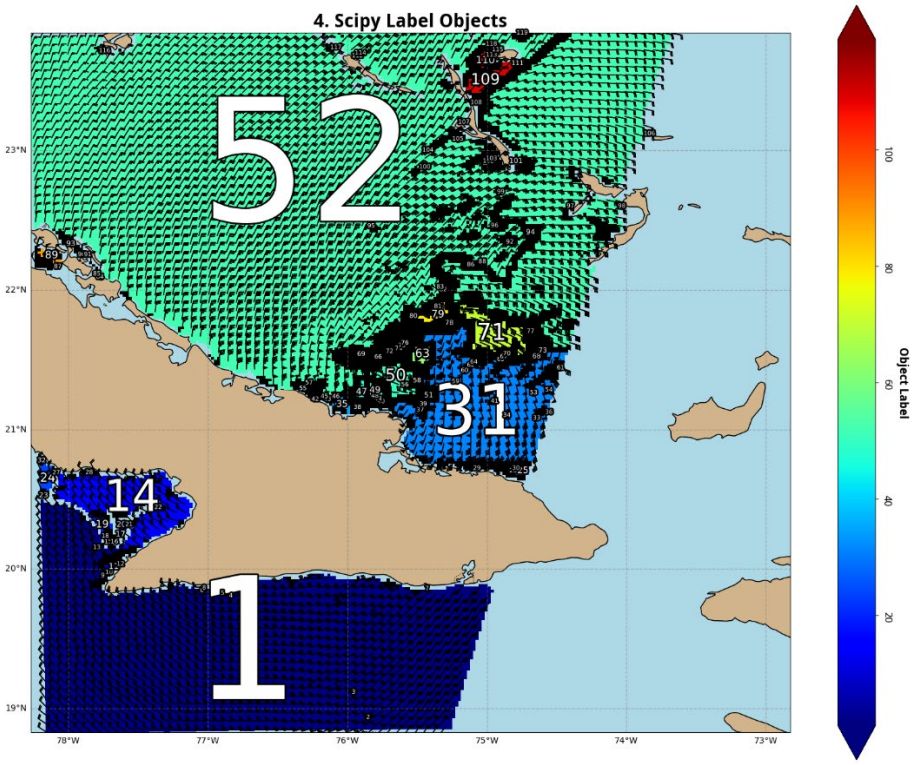

Figure 2 ASCAT-B pass over Melissa on October 29th, 2025. The image is the result of applying the SciPy's scipy.ndimage.label to the "Negative Threshold" mask. Win barbs indicate general wind direction for each object. The white numbers show label number for each object, with the size varying based on the population of WVCs in the group.

3.5. Object Statistics Computation

For each labeled object, two populations are characterized: the interior (object) cells and the immediately adjacent boundary (edge) cells. The object boundary is identified by convolving the binary object mask with a cross-shaped 3×3 kernel:

$$K = [[0,1,0],[1,1,1],[0,1,0]] \quad (8)$$

Cells outside the object where the convolution result is ≥1.0 (indicating adjacency to at least one object cell) and that are also outside the agreement mask constitute the object's edge population. The following metrics are computed for each object: object circular mean, 5th and 95th circular percentiles, quantile range, edge circular mean, edge 5th and 95th percentiles, edge count, object count, and the average angular difference between the object's wind directions and the orthogonal reference field.

3.6. Verification Tests

Each labeled object is subjected to three independent verification tests. An object is rejected by the filter (is labeled as an anomaly) if all three tests pass.

3.6.1. Consistency Test (Similarity)

This test verifies that the object's wind direction distribution is consistent with its surrounding edge. The object's 5th percentile must fall within a buffer below the edge's 5th percentile, and the object's 95th percentile must fall within a buffer above the edge's 95th percentile:

$$edge_{q05} - B \leq obj_{q05} \quad AND \quad obj_{q95} \leq edge_{q95} + B \quad (9)$$

where B is the quantile range buffer (default: 20.0°). This test identifies objects whose wind directions are systematically offset from the surrounding field. If the edge and object are not consistent with one another, they cannot be reliably labeled as anomaly. This test is generally more of formality to make sure the earlier steps are working. It is rare for an object to not pass this test.

3.6.2. Q-Range Test

This test verifies that the internal directional spread of the object is below the quadrant threshold: $q_{range} < \tau_{quad}$ (default: 90.0°), where q_{range} is the difference between obj_{q95} and obj_{q05}

$$q_{range} < \tau_{quad} \text{ (default: 90°)}, \quad \text{where } q_{range} = obj_{q95} - obj_{q05} \quad (10)$$

This test is employed for the purpose of interpolation. Objects that are below 90° can be interpolated very easily, but exceeding 90° contain wind directions spanning more than one quadrant and cannot be reliably interpolated in later processing steps.

3.6.3. Orthogonal Test

An orthogonal reference field is generated by computing the direction perpendicular to the vector pointing from the storm center to each WVC, representing the expected tangential flow in a cyclonic vortex. The result is counter-clockwise for the northern hemisphere and clockwise for the

southern hemisphere. The average angular difference between the object's wind directions and the reference orthogonal field must exceed the orthogonal threshold:

$$\bar{\alpha}\left(\Delta\alpha(\alpha_{raw}, \alpha_{orth})\right) > \tau_{orth}(default: 45°) \quad (11)$$

Objects that differ from the expected circulation by more than τ_{orth} are considered highly aliased.

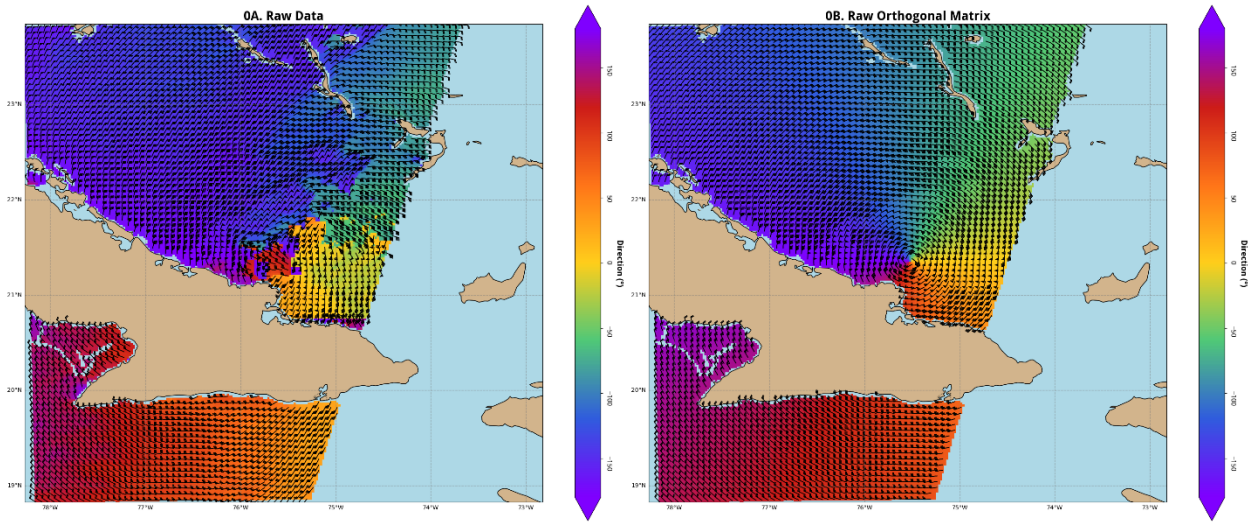

Figure 3 ASCAT-B pass over Melissa on October 29th, 2025. (Left) The colormap shows the raw data with wind barbs indicating the vector direction and magnitude. (Right) The colormap shows a representation of ideal circulation with wind barbs indicating the vector direction and magnitude. The magnitudes for the wind barbs in are the same in both plots. The difference between

3.7. Mask Generation

Objects that pass all three tests are flagged as anomalous. The final binary mask marks all cells belonging to anomalous objects (value = 1) and retains all cells belonging to verified objects (value = 0). NaN-valued cells in the original wind direction field are excluded from the mask.

3.8. Algorithm Parameters

Table 1. Anomaly Detection Algorithm Parameters

Parameter	Symbol	Default	Description
Difference Threshold	τ_{diff}	7.5°	Maximum local difference for agreement regions
Quadrant Threshold	τ_{quad}	90.0°	Maximum internal q-range for valid objects
Orthogonal Threshold	τ_{orth}	45.0°	Minimum orthogonal deviation for valid objects
Q-Range Buffer	B	20.0°	Tolerance buffer for consistency test bounds

Table 1 All the adjustable values in Section 3.

Section 4
Wind Direction Interpolation

4.1. Overview

After anomalous wind directions have been identified and masked, the flagged cells must be filled with physically plausible wind direction estimates. All interpolation operations are performed in the complex exponential domain (Section 2.1.1) to correctly handle the circular nature of wind directions.

4.2. Two-Dimensional Griddata Interpolation

For general 2D gap-filling, SciPy's griddata function is applied with a linear interpolation method. The valid (non-NaN) wind directions are converted to complex exponentials, and their grid coordinates serve as the interpolation nodes. The NaN and invalid non-NaN locations provide the query points for interpolation. The interpolated complex values are converted back to angular degrees. This method fills interior gaps effectively but can only extrapolate when query points are located in between valid data points.

4.3. Radial Basis Function (RBF) Edge Interpolation

To handle edge regions and gaps near swath boundaries where griddata extrapolation fails, an RBF interpolation method is applied using SciPy's RBFInterpolator with a linear kernel. The number of nearest neighbors varies: 5 for the initial pass, 12 for the final iterative pass. The RBF method provides smooth extrapolation beyond the convex hull of valid data, making it suitable for filling gaps at swath edges. All operations are performed in the complex exponential domain.

4.4. Interpolation Sequence

In the single-pass processing mode, griddata interpolation is applied first, followed by RBF edge interpolation to fill any remaining gaps. In the iterative processing mode (Section 7), only 2D griddata interpolation is used during intermediate iterations, with the final RBF edge interpolation applied after convergence using an expanded neighborhood of 12 nearest neighbors.

Section 5
Ambiguity Re-Selection

5.1. Selection Algorithm

After interpolation produces a spatially continuous guide field, the algorithm re-selects wind direction ambiguities by finding the ambiguity that minimizes the angular distance to the interpolated guide field at each flagged WVC. For each cell, the algorithm computes:

$$k* = argmin_k \left|\Delta\alpha\left(\alpha_{amb}^k, \alpha_{interp}\right)\right| \quad (12)$$

A threshold of 15.0° is appended as a fifth option (index 4). If no ambiguity falls within 15° of the interpolated direction, the interpolated direction itself is retained as the selected wind direction. This fallback mechanism preserves the smooth interpolated field when none of the original ambiguities are sufficiently close.

5.2. Selection Outputs

The ambiguity selection produces a 2D array of integer indices (0-3 for the four ambiguities, 4 for the interpolated direction). For cells with index 0–3, the corresponding ambiguity wind direction replaces the interpolated value, providing a discrete direction from the original GMF inversion while maintaining spatial coherence with the guide field. When the index is 4, the interpolated wind direction is retained and a new wind speed needs to be calculated as outlined in section 6.

Section 6
Wind Speed Retrieval

6.1. CMOD5.h Geophysical Model Function

The CMOD5.h Geophysical Model Function (GMF) relates the C-band normalized radar cross section (NRCS) to the near-surface wind vector and radar geometry (Soisuvarn, CMOD5.H—A High Wind Geophysical Model Function for C-Band Vertically Polarized Satellite Scatterometer Measurements, 2013). The GMF is implemented as a three-dimensional lookup table parameterized by: wind speed (0.2 to 50.0 m/s, step 0.2 m/s, 250 bins), incidence angle (16.0° to 66.0°, step 1.0°, 51 bins), and wind-relative azimuth (0.0° to 180.0°, step 2.5°, 73 bins).

Table 2. CMOD5.h GMF Lookup Table Dimensions

Parameter	Minimum	Maximum	Step	N Bins
Wind Speed (m/s)	0.2	50.0	0.2	250
Incidence Angle (°)	16.0	66.0	1.0	51
Wind-Relative Azimuth (°)	0.0	180.0	2.5	73

Table 2 Outlines the grid values of CMOD5.h.

6.2. Wind Speed Inversion

Given the corrected wind direction and the measured σ_0 values from the three ASCAT beams, the wind speed is retrieved by inverting the GMF. For each beam, the expected σ_0 is computed as a function of wind speed (at the known incidence angle and corrected wind-relative azimuth). The squared differences between measured and modeled σ_0 values are summed to form a Maximum Likelihood Estimation (MLE) cost function:

$$MLE(v) = \sum_{k=1}^{3} [\sigma_k^0 - GMF(v, \varphi_k, \theta_k)]^2 \quad (13)$$

where v is wind speed, φ_k is the wind-relative azimuth for beam k, and θ_k is the incidence angle. The measured σ_0 values are converted from dB to linear units prior to comparison. The minimum of the MLE cost function is found by evaluating the cost function at each wind speed bin, constructing a cubic spline interpolant, evaluating at fine resolution (0.001 m/s steps), and selecting the wind speed at the global minimum.

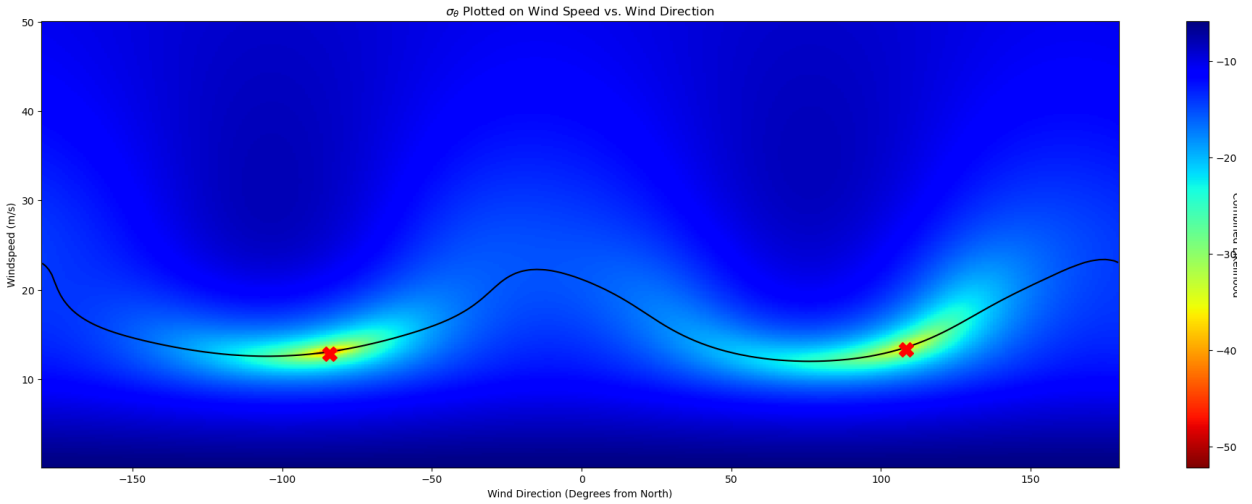

Figure 4 A visual of σ_0 for each windspeed vs wind direction. The brighter colors indicate valleys in the colormap where the most likely combinations of wind speed wind direction occur. The black line is the most likely windspeed value for each wind direction value.

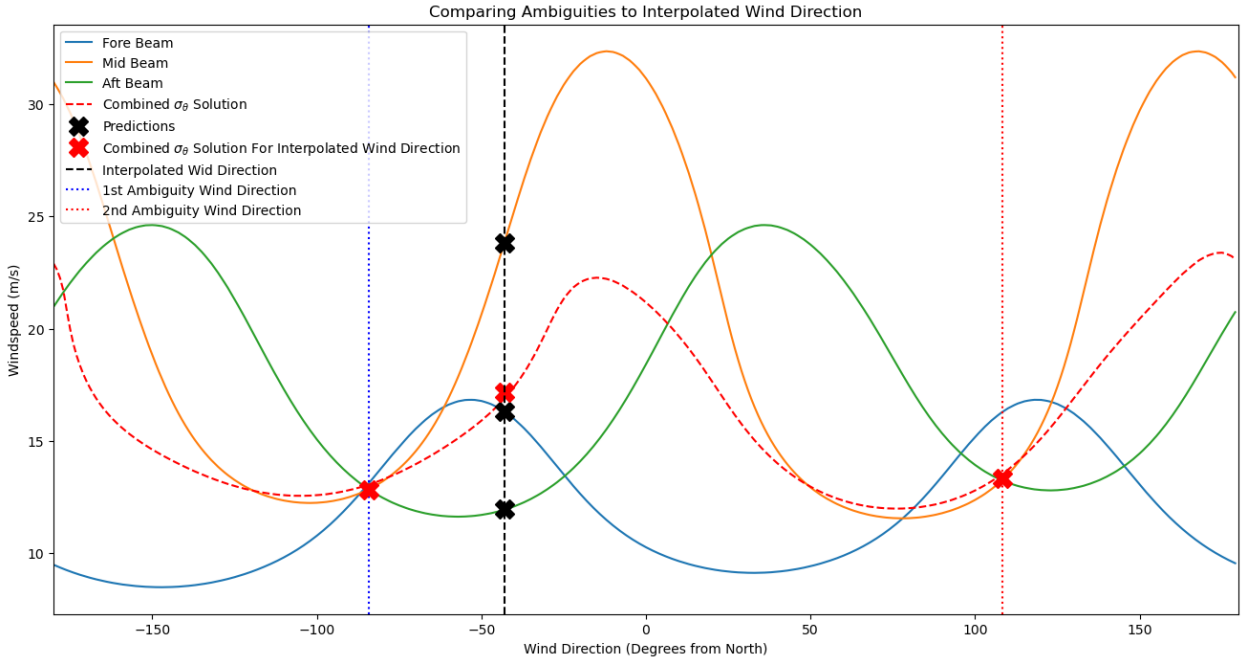

Figure 5 Plot of the ambiguity curve for each beam: Fore (blue), Mid (orange), Aft (green). The three σ_0 curves are combined into one solution (red). The interpolated wind direction is shown as a black dashed line with black "X"s indicating the associated wind speed for each ambiguity and red "X" indicating the most likely wind speed for the interpolated wind direction. Blue and red dotted lines indicate the wind directions of the 1st and 2nd ambiguities, with red "X"s indicating their respective most likely wind speeds.

6.3. UHR Wind Speed Scaling

The raw retrieved wind speeds are scaled using a rational polynomial correction to account for UHR processing characteristics:

$$v_{scaled} = \frac{P_{up}(v)}{P_{down}(v)} \tag{14}$$

where P_{up} and P_{down} are 5th-degree polynomials with empirically determined coefficients. This correction adjusts the UHR wind speed distribution to match the standard ASCAT wind product.

Table 3. UHR Wind Speed Scaling Polynomial Coefficients

Polynomial	c0	c1	c2	c3	c4	c5
P_{up}	−0.0443	1.0578	−0.1012	0.00651	−3.42e–4	8.84e–6
P_{down}	1.0000	−0.0811	0.00377	−1.82e–4	5.57e–6	−2.91e–10

Table 3 5th degree polynomial coefficients for P_{up} and P_{down}.

6.4. Final Wind Speed Retrieval

The complete retrieval integrates multiple wind speed sources: (1) for cells where an original ambiguity was selected (indices 0–3), the corresponding ambiguity wind speed from the original retrieval is used after applying the UHR scaling polynomial; (2) for cells where the interpolated direction was selected (index 4), a new wind speed is retrieved from the σ_0 measurements using GMF inversion, followed by UHR scaling and unit conversion to knots; (3) cells that were originally NaN remain NaN in the output.

Section 7
Iterative Processing Pipeline

7.1. Rationale

A single pass of the anomaly detection and correction pipeline may not resolve all directional errors, particularly in complex wind patterns where anomalous regions are adjacent to or partially overlap with other anomalous regions. The iterative pipeline applies the filtering, interpolation, and ambiguity selection steps repeatedly until convergence.

7.2. Convergence Criteria

The iterative loop terminates when one of the following conditions is met: (1) Convergence: the wind direction field from the current iteration is within 1.0° of the previous iteration at all cells (using numpy.allclose with atol=1.0 and equal_nan=True); (2) Maximum iterations: the loop has executed 10 iterations; (3) Complete masking: the cumulative change mask covers all cells.

7.3. Iteration Procedure

Each iteration proceeds as follows: (1) Apply the contour filter to the current wind direction field, producing a filter mask; (2) Accumulate the filter mask into the cumulative change mask via logical OR; (3) Set filtered cells to NaN and apply 2D griddata interpolation; (4) Re-select ambiguities using the interpolated guide field; (5) Construct the updated wind direction field from selected ambiguities and interpolated values; (6) Check convergence and either terminate or proceed.

7.4. Post-Convergence Processing

After the iterative loop converges, a final RBF edge interpolation is applied with 12 nearest neighbors to smooth any remaining edge artifacts. A final ambiguity re-selection is performed against this smoothed field. The resulting wind directions are used for the final wind speed retrieval.

7.5. End-to-End Pipeline Summary

Table 4. End-to-End Processing Pipeline Steps

Step	Operation	Method
1	Storm center location	IBTrACS interpolation via scipy.interpolate.interp1d
2	Data extraction and cropping	Configurable crop radius around storm center
3	Orthogonal reference field	Geometric computation from storm center coordinates
4	First-pass contour filter	Anomaly detection (Section 3)
5	First-pass interpolation	Griddata + RBF edge interpolation (Section 4)
6	First-pass ambiguity selection	Angular distance minimization (Section 5)

Step	Operation	Method
7	First-pass wind speed retrieval	GMF inversion (Section 6)
8	Iterative filtering loop	Repeated Sections 3–5 until criteria is met
9	Final RBF edge interpolation	RBF with 12 neighbors
10	Final ambiguity re-selection	Section 5
11	Final wind speed retrieval	Section 6
12	Output generation	Interpolated NetCDF + diagnostic plots

Table 4 A step by step outline of the processing steps taken in iterative quality control pipeline.

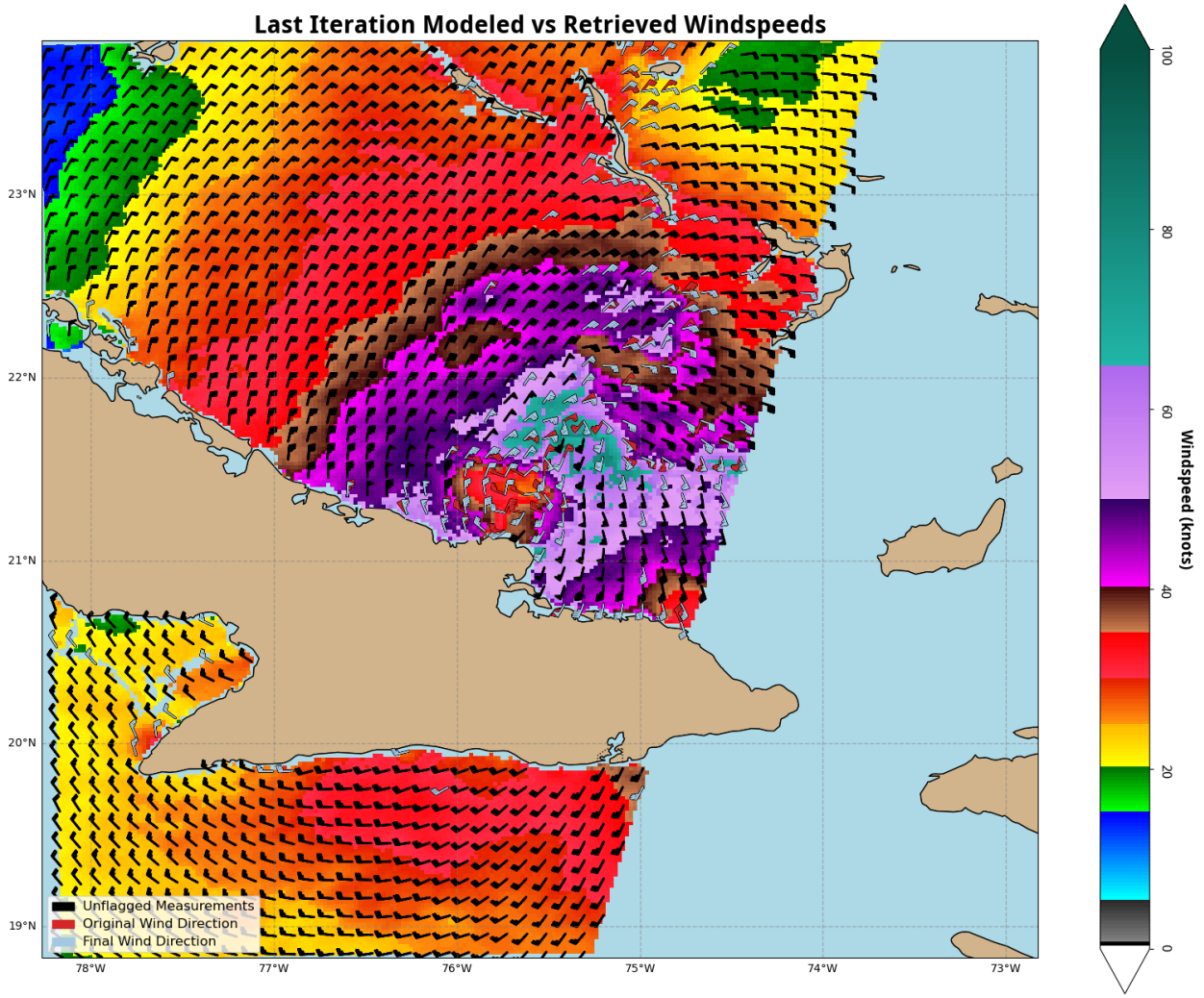

Figure 6 ASCAT-B pass over Melissa on October 29th, 2025. The plot shows the wind speed in knots for each WVC via the colormap as indicated by the colorbar. The wind barbs show the direction and magnitude of the hurricane. Black wind barbs indicate measurements that were never labeled as anomalous. Red wind barbs represent the original value of the anomalous WVCs. Greyish blue wind barbs represent the corrected value of the anomalous WVCs. Overlapping red and greyish blue mean the corrected and original value are the same.

Section 8
Storm Center Location

8.1. IBTrACS Best Track Data

The International Best Track Archive for Climate Stewardship (IBTrACS) dataset provides historical tropical cyclone best track information including storm center positions (latitude, longitude) at 6-hourly intervals (Knapp, 2010). The evaluation pipeline uses IBTrACS v04r01 for storm center estimation.

8.2. Temporal Interpolation

Since ASCAT pass times do not generally coincide with IBTrACS reporting times, the storm center position is interpolated to the mean observation time of the ASCAT pass. The latitude and longitude time series are independently interpolated using SciPy's 1D linear interpolation with extrapolation enabled, applied to Unix epoch timestamps for numerical stability. The interpolated storm center is matched to the nearest WVC in the ASCAT grid by computing the Euclidean distance between the interpolated center coordinates and all grid cell coordinates.

8.3. Orthogonal Reference Field

The orthogonal reference field represents the expected tangential flow direction at each WVC assuming cyclonic circulation. For each cell, the vector from the storm center to the cell is computed, and the perpendicular (counter-clockwise) direction is taken as the reference:

$$\alpha_{\text{orth}} = \begin{cases} \text{atan2}(dx, -dy), if\ in\ Northern\ Hemisphere \\ \text{atan2}(-dx, dy), if\ in\ Southern\ Hemisphere \end{cases} \quad (15)$$

where dx and dy are the longitude and latitude offsets from the storm center. A coordinate transformation is applied to convert from mathematical convention to meteorological convention (direction from which the wind blows).

8.4. Automated Center Fixing (Beta Tests)

Active research is taking place to develop an autonomous center fix for ASCAT UHR passes. This would enhance the Near Real Time (NRT) deployment of the entire algorithm. IBTrACS has center fix estimates are frequently aliased from the ground truth hurricane centers. Even small errors in the center fix can drastically hurt the results of the algorithm. A center fix tailored to each ASCAT UHR pass enhances the quality control pipeline and upgrades the fidelity of ASCAT UHR data.

Section 9
Validation and Test Cases

9.1. Test Dataset

The algorithm has been evaluated on a dataset of 22 ASCAT UHR tropical cyclone passes spanning 7 named storms from the 2024–2025 hurricane seasons:

Table 5. Validation Storm Dataset

Storm	Year	Passes	Instruments
Erin	2025	7	ASCAT-B, ASCAT-C
Helene	2024	1	ASCAT-C
Keli	2025	1	ASCAT-B
Kristy	2024	1	ASCAT-C
Melissa	2025	7	ASCAT-B, ASCAT-C
Milton	2024	4	ASCAT-B, ASCAT-C
Ragasa	2025	1	ASCAT-B

Table 5 Overview of the case study storm passes. This table includes the name of each storm, the year of the storm, the number of passes from a storm, and which ASCAT instrument(s) captured the pass.

Each test case includes ascending and descending passes from both ASCAT-B and ASCAT-C instruments, providing diverse viewing geometries and wind field configurations. The crop radius for each storm is individually configured based on storm size, ranging from 25 to 125 WVCs.

9.2. Diagnostic Outputs

For each processed storm pass, the pipeline generates: (1) Interpolated NetCDF files containing original and corrected wind fields plus ambiguity selection indices; (2) Over 15 diagnostic visualization panels including original wind barbs, σ_0 quality metrics, masked wind fields at each iteration, nearest ambiguity wind barbs, ambiguity selection colormaps, wind speed and direction bias maps; and (3) HTML log files documenting per-object statistics and verification test results at each iteration.

9.3. Quality Metrics

The following per-WVC quality metrics are preserved in the output files for downstream analysis: σ_0 fore-aft difference (sigfa_diff) as an indicator of cross-track calibration consistency; the Maximum Likelihood Estimator (MLE) for goodness-of-fit; model speed bias (difference between retrieved UHR and L2B model wind speed); rain flag (QC flag bit 12); and ambiguity selection index (0–4).

Section 10
References

References

EUMETSAT. (2014). *Metop-A ASCAT L1 Data Record Release 2 (CF-003): User Guide.* Darmstadt, Germany: European Organisation for the Exploitation of Meteorological Satellites. Retrieved from https://user.eumetsat.int/s3/eup-strapi-media/pdf_ma_ascat_l1_cdr_003_user_guide_a6c37bce29.pdf

Knapp, K. (2010). The International Best Track Archive for Climate Stewardship (IBTrACS): Unifying Tropical Cyclone Data. *91*(3), 363 - 376. doi:10.1175/2009BAMS2755.1

Lindsley, R. (2010). Adapting the sir algorithm to ASCAT. 3402-3405. doi:10.1109/IGARSS.2010.5650207

Soisuvarn, S. (2013). CMOD5.H—A High Wind Geophysical Model Function for C-Band Vertically Polarized Satellite Scatterometer Measurements. *51*(6), 3744-3760. doi:10.1109/TGRS.2012.2219871

Soisuvarn, S. (2023). High-Resolution Coastal Winds From the NOAA Near Real-Time ASCAT Processor. *61*, 1-12. doi:10.1109/TGRS.2023.3279764